

Maintaining Constant Pulse-duration in Highly Dispersive Media using Nonlinear Potentials

*Haider Zia **

Haider Zia

University of Twente, Department Science & Technology, Laser Physics and Nonlinear Optics Group, MESA+ Research Institute for Nanotechnology, Enschede 7500 AE, The Netherlands

E-mail: h.zia@utwente.nl

Keywords: cross-phase modulation, stationary pulses, ultrafast pulses, higher-order dispersion, pulse trapping, solitons, nonlinear schrödinger equation

Abstract

A method is shown for preventing temporal broadening of ultrafast optical pulses in highly dispersive and fluctuating media for arbitrary signal-pulse profiles. Pulse pairs, consisting of a strong-field control-pulse and a weak-field signal-pulse co-propagate, whereby the specific profile of the strong-field pulse precisely compensates for dispersive phase in the weak pulse. A numerical example is presented in an optical system consisting of both resonant and gain dispersive effects. Here we show signal-pulses that do not temporally broaden across a vast propagation distance, even in the presence of dispersion that fluctuates several orders of magnitude and in sign (for example within a material resonance) across the pulse's bandwidth. Our approach illustrates the potential for using cross-phase modulation to compensate for dispersive effects on a signal-pulse and fills the gap in the current understanding of this nonlinear phenomenon.

Introduction

The rich and complex physics of soliton formation has been a central topic in ultrafast optical physics since the early 1970s when Akira Hasegawa first suggested that temporal solitons could exist in anomalous optical fibers.^[1,2] The initial allure of optical solitons was the prospect of a

substantial improvement of data transmission rates in optical fiber communications since dispersive effects would not distort and smear out the solitary optical waveforms.

Optical solitons are also used in many bridging studies between the various fields of physics, such as optical analogs of bound states and Bose-Einstein condensates and even the simulation of black hole event horizons.^[3-5] While higher-order solitons have wide use in nonlinear optics, such as in supercontinuum generation^[6-9] and nonlinear pulse compression,^[10-13] they are unstable and usually decay to fundamental solitons.^[14] The fundamental soliton provides the most appeal, as its amplitude profile in the temporal domain does not change as it propagates.

However, the fundamental soliton is highly specific in waveform and is only stable under slow-varying group-velocity dispersion. I.e., the soliton profile must be a hyperbolic secant and its energy must satisfy specific material conditions.^[14] The profile specificity presents limitations in potentially lucrative optical applications for solitons. For example, it would sometimes be more beneficial for optical waveforms that are not hyperbolic secant profiles, e.g., Gaussian pulses, to propagate in dispersive media without temporally broadening.

Recently, this problem has been somewhat resolved as soliton solutions in the presence of even higher-order dispersion terms have been analytically found and experimentally demonstrated.^[15] Nevertheless, while the choice of pulse profiles is now larger, it can still only be one of specific profiles. As well, to exploit these higher-order dispersion solitons, other dispersion terms cannot be present past a perturbative degree. For example, the so-called quartic soliton must only be accompanied by a nonzero 4th order group-velocity dispersion (GVD) coefficient.

Given the above discussion, it would be highly beneficial to obtain a method to generate stationary or close to stationary pulse profiles (i.e., where the shape of the pulse and its duration remains approximately the same for the entire propagation) for a more significant amount of pulse shapes and dispersion profiles. The technique would enable, for example, pulses that could be guided through turbulent group-velocity dispersion that fluctuates both in sign and in

orders of magnitude without broadening. Examples of turbulent dispersive media are widespread in optics and they include resonant loss and gain media, Raman active materials and past the photonic bandgap of Bragg grating structures.^[16–20] Another application could be to prevent temporal broadening of complicated single-photon wavefunction shapes (that are far from hyperbolic-secants) such that dispersive effects are negligible in resonator configurations used as quantum memory.^[21–22]

In this paper, we formulate and show, through numerical examples, a method to prevent temporal broadening of pulses of more arbitrary shapes in a manner less dependent on the waveguide's dispersion profile than current soliton generation allows. We do this by controlling a weak-amplitude signal-pulse with a 'control' pulse that offers an optical potential that induces cross-phase modulation (XPM).

XPM has been explored before in the context of solitons, for example, in generating (second-order dispersion) soliton pairs across dispersion regions, i.e., a dark soliton in normal dispersion and a bright soliton in anomalous dispersion that is sustained through XPM. Cross-phase modulation has also been extensively explored in the context of continuously shifting the wavelength of a pulse or a dispersive narrowband spectral component in a technique called optical trapping.^[23–28]

While these formative experiments are significant to study XPM and enable new applications, they do not overcome the pulse profile specificity needed. For either the control or signal-pulse or both a highly specific profile, such as a fundamental soliton profile, or a truncated Airy function^[29] must be present. Also, these approaches only work with dominant second-order group-velocity dispersion, where other dispersive terms are negligible.

As opposed to the previous literature that primarily focused on the frequency effects of XPM or interaction dynamics of specific pulse shapes, our focus here is to use XPM to limit the temporal broadening of a general signal-pulse in a general dispersion profile. The analytic expression for the exact control-pulse profile needed given an arbitrary or general signal-pulse

profile is obtained for the first time. The control-pulse shape is obtained that would generate the conjugate temporal phase to the one from dispersion, such that the two cancels to zero for the signal-pulse.

Ultimately this allows for near invariant temporal solutions across a wide range of signal-pulse shapes and dispersion profiles. The method then alleviates the burden of trial-and-error methods to find the proper control-pulse profile and fills the gap in our understanding of XPM induced control of temporal broadening.

1. Theoretical Description

We start by deriving the method's expressions used to obtain the control-pulse needed for maintaining a stationary signal-pulse. We restrict our analysis to the waveguide case, where only the propagation spatial dimension needs to be considered. The nonlinear equations of motion of two pulses, separated in central frequency or polarization, with complex envelope functions u_1 (control-pulse) and u_2 (signal-pulse) undergoing XPM is given in **Equations (1)** and (2):[30]

$$\begin{aligned} \frac{\partial u_1}{\partial z} &= \sum_{k \geq 2} \frac{i^{k+1}}{k!} \beta_k \frac{\partial^k}{\partial T^k} u_1 + i\gamma[|u_1|^2 + 2|u_2|^2]u_1 \\ \frac{\partial u_1}{\partial z} &\approx \sum_{k \geq 2} \frac{i^{k+1}}{k!} \beta_k \frac{\partial^k}{\partial T^k} u_1 + i\gamma[|u_1|^2]u_1 \end{aligned} \quad (1)$$

$$\begin{aligned} \frac{\partial u_2}{\partial z} &= \sum_{k \geq 2} \frac{i^{k+1}}{k!} \kappa_k \frac{\partial^k}{\partial T^k} u_2 + i\gamma[|u_2|^2 + 2|u_1|^2]u_2 \\ \frac{\partial u_2}{\partial z} &\approx \sum_{k \geq 2} \frac{i^{k+1}}{k!} \kappa_k \frac{\partial^k}{\partial T^k} u_2 + i\gamma[2|u_1|^2]u_2 \end{aligned} \quad . \quad (2)$$

we impose that $|u_1|$ is much larger than $|u_2|$ and that the signal-pulse has a small amplitude such that it does not contribute to any nonlinear effects. Therefore, Equations (1) and (2) reduce to

the indicated approximate forms. β_k , κ_k are the dispersive coefficients, arising from the frequency-dependent wavenumber Taylor expanded about the control or signal's central frequency ω_1 or ω_2 . T is the pulse time-coordinate defined in a co-moving frame-of-reference.

The above system-equations are solved to obtain the control-pulse envelope profile giving a stationary solution of the signal-pulse. However, a few conditions must be met, which we list before indicating the derivation:

1. The dispersive broadening of the control-pulse must be negligible, i.e., the dispersion

length, usually approx. proportional to $\frac{1}{\beta_2}$ [6], must be larger than the interaction length of the two pulses.

2. The group-velocities of both pulses, u_1 and u_2 are the same. This means that the group-

delay at the control-pulse's central frequency, i.e., $\frac{\partial k}{\partial \omega}|_{\omega_1}$ where k is the wavenumber, must equal to that of u_2 .

The ideal group-delays of the pulse-pair then satisfy,

$$\int_{\omega_0}^{\omega_1} \tilde{D}_1 d\omega = \int_{\omega_0}^{\omega_2} \tilde{D}_2 d\omega \quad . \quad (3)$$

Where \tilde{D}_1 , \tilde{D}_2 are the frequency dependent group-velocity dispersion seen by the control and signal-pulse in **Equation** (3). ω_0 is the frequency corresponding to the group-velocity of the common moving time frame-of-reference of the two pulses. We take a frame-of-reference co-moving and centered with the control-pulse (i.e., ω_0 is the control-pulse's central frequency).

1.1. Control-pulse Formulation

The first step in formulating the required control-pulse is to insert the following Ansatz $u_2(T, z) = u_2(T, z=0)e^{ipz}$ (p is a constant) into Equation (2). The approximation : $u_1(T, z) = u_1(T, z=0)e^{i\gamma|u_1|^2 z}$ is also inserted –which is exact if there is no dispersive broadening for the control-pulse. Dividing out common terms, this yields

$$|u_1(T, z=0)|^2 = \frac{1}{2\gamma} \left[p - \frac{1}{u_2(T, z=0)} \sum_{k \geq 2} \frac{i^k}{k!} \kappa_k \frac{\partial^k}{\partial \tau^k} u_2(T, z=0) \right]. \quad (4)$$

Since the left-hand side of **Equation** (4) equates to a positive definite function for all T , so must the right-hand side. From this positive definitive condition, p is a real constant and it can be shown that the signal-pulse must always be in a form $u_2(T, z=0) = f(T)e^{i\nu T}$ where $f(T)$ is a transform limited complex amplitude function and ν is a constant. Generally,

$$p \geq \max \left[\frac{1}{u_2(T, z=0)} \times \sum_{k \geq 2} \frac{i^k}{k!} \kappa_k \frac{\partial^k}{\partial \tau^k} u_2(T, z=0) \right], \text{ to guarantee that the left-hand side can never be negative.}$$

It seems mathematically, that another condition needed for Equation (4) to be valid is that the odd-dispersion coefficients must be zero, at least, for the dispersion profile that covers the signal-pulse's bandwidth. Thus, across the bandwidth of the signal-pulse, the dispersion profile

is ideally symmetric about the central wavelength. However, we find from full numerical simulations that this condition is not strictly necessary and introduces little error for moderate third-order dispersion if Equation (4) is modified to Equation (5) given as:

$$u_1(T, z=0) = \sqrt{\frac{1}{2\gamma} \left[p - \frac{1}{u_2(T, z=0)} \sum_{k \geq 2} \frac{i^k}{k!} \beta_k \frac{\partial^k}{\partial \tau^k} u_2(T, z=0) \right]} , \quad (5)$$

even if this modification is not supported mathematically.

Equation (4) indicates that $u_1(T, z=0)$ can be a product between any real function and exponential phase function since only the absolute magnitude must obey the equation. Values of T that lie outside of the temporal profile of the signal-pulse, $u_1(T, z=0)$ can equal zero or any convenient function without additional error.

1.2. Deviation From Stationary Propagation

In a practical setting, since Equation (4) consists of a quotient term, it may be necessary to truncate it for large T when $u_1(T, z=0)$ goes to zero. The truncation is decided by the desired energy upper bound that the control-pulse must satisfy. Thus, $u_1(T, z=0)$ is uncontrolled for T larger than the truncation window, yielding the potential error of dispersive broadening in the wings of the signal-pulse.

For example, it can be shown that for a Gaussian pulse, $u_1(T, z=0) = Ae^{-\frac{T^2}{2T_o^2}}$, Equation (4) becomes

$$|u_1(T, z=0)|^2 = \frac{1}{2\gamma} \left[p - \sum_{k \geq 2} \frac{i^k}{k!} \kappa_k H_{e_k} \right] , \quad (6)$$

where H_{e_k} are the set of Physicists Hermite Polynomials^[31] of order k .

When only second-order group-velocity dispersion is present, **Equation (6)** equates to a parabolic function, and therefore, does not converge uniformly to zero. Thus, the edges of a Gaussian pulse may temporally disperse away from the XPM controlled central region of the signal-pulse. This limitation will be explored in the subsequent section.

2. Near Stationary Pulses in Turbulent Dispersive Media

To understand both the limitations and impact of the above theoretical procedure for XPM induced stationary pulse propagation, we consider pulse propagation in a turbulent dispersive waveguide medium. We restrict our analysis to the waveguide case, as diffraction is negligible and can be omitted from the analysis. The diffractive term of the full three-dimensional NLSE, for example shown in [32] cannot be accounted for by method used to obtain Equation (4).

To solve for the dynamics of the pulses undergoing nonlinear propagation in the turbulent waveguide, we first use Equation (5) to generate the amplitude function of the control-pulse given a certain signal-pulse we want to propagate invariantly. We then numerically solve, using the split-step Fourier method, [30] the coupled NLSE equations (Equations (1) and (2)) for both pulses, with the input control and signal profile as initial conditions.

The turbulent dispersive waveguide medium we study is defined as having narrow fluctuations between positive and negative GVD spanning orders of magnitude within a small bandwidth of frequencies. We apply our method for turbulent dispersion because the highly fluctuating dispersion demonstrates the full effectiveness and potential for our method, i.e., the large dispersion fluctuations would make controlling the associated dispersive effects challenging. While we show our method in this extreme case, we find our method is effective for more moderate examples too, such as pulse propagation through a telecom fiber with modest higher-order dispersion.

Impactful examples of such highly fluctuating dispersion that occur in many optical applications are generally when the frequency range of a pulse covers a waveguide's absorption dip and/or gain peak or covers waveguide resonances, e.g., from leaky modes or evanescent coupling to neighboring waveguides. Such a case can occur for an ultrafast pulse (i.e., covering a large bandwidth) traveling through a doped waveguide that amplifies light while also coupled to a ring resonator detuned from the gain profile.^[17] Another significant case is when a pulse travels in a waveguide where the Stokes peak location and absorption dip location (Stokes-shift) from the Raman effect are situated within the bandwidth of the original pulse.^[19]

To illustrate the control of temporal broadening within turbulent dispersive media, we have constructed an artificial waveguide that possesses a weak absorption and gain resonance characteristic of leaky mode strand resonances in photonic crystals.^[33] The features are characterized by a Lorentzian gain peak and absorption dip within the bandwidth of an ultrafast (200 fs) pulse, where the pulse has a carrier frequency that sits precisely at the midpoint of these features. We take as the Lorentzian parameters used, the typical values from leaky mode strand resonances in photonic crystal fibers given in^[33]. While we show an example with only two resonant features, we have also studied waveguides consisting of a series of multiple resonances, whereby the pulse bandwidth is centered such that the dispersion profile is symmetric within its bandwidth.

The waveguide has a flat-zero GVD when the absorption and gain are neglected. Through the associated Kramers-Kronig relations, the group-velocity dispersion is derived in the waveguide and is shown in **Figure 1a** along with the signal and control's normalized spectral energy density distributions. The dispersion is symmetric around the signal-pulse's carrier frequency and fluctuates over five orders of magnitude.

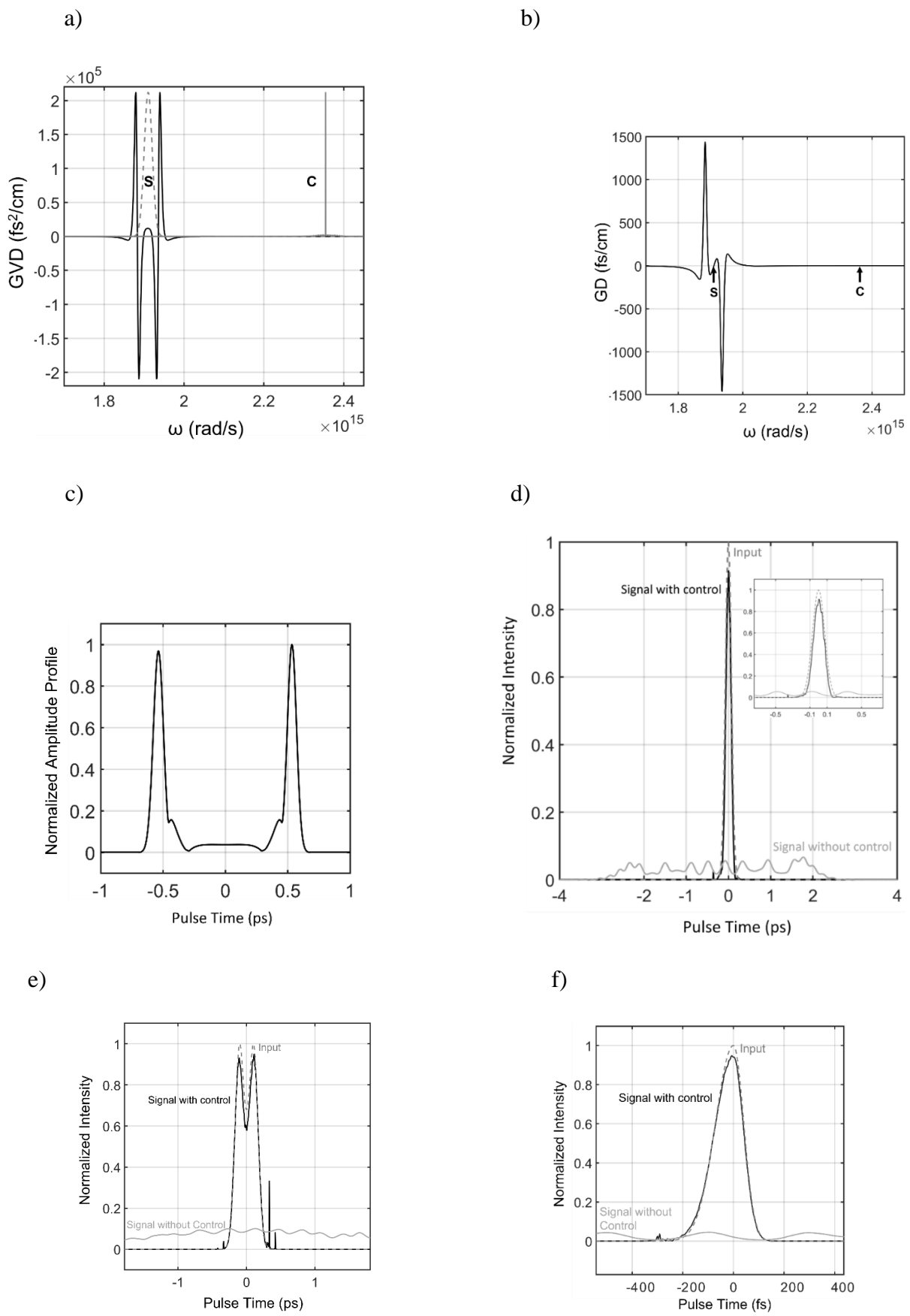


Figure 1. a) Group-velocity dispersion versus angular frequency with signal (s) and control (c) normalized spectral-density-distributions indicated in gray. b) Frequency-dependent group-delay with signal and control-pulse locations indicated. c) Amplitude of control-pulse versus pulse time. d) Normalized-to input-peak intensity distribution versus pulse-time for signal without control, signal with control and input profile. Inset is a zoom-in around the controlled signal-pulse.

The interaction of the highly fluctuating dispersion with our set of signal-pulses provides a stringent test for how well the XPM modulated signal-pulse avoids temporal broadening. To evaluate the quality of the controlled signal-pulse we compare it to the signal's temporal profile when there is no control-pulse. This comparison is done for three different signal-pulse types to show that our method works for arbitrary signal-pulses.

To isolate the dynamics of the signal-pulse, we center the control-pulse in a zero-dispersion region such that dispersive distortion of the amplitude profile is not present. As well, both signal and pulse propagate at approx. the same group-velocity with negligible walk-off as shown in the group-delay versus frequency, i.e., **Figure 1b**. The amplitude profile of the control-pulse is shown in **Figure 1c**, with an energy of approx. 11 μJ . In general, we find that the control-pulse energy scales directly with the order of magnitude of the dispersion fluctuations, going to below nJ's for dispersion fluctuations on the order of unity.

We now proceed with our first signal-pulse example, which is a 200 fs Gaussian pulse. After 25 cm of propagation in the medium, the XPM controlled signal-pulse remains close to the Gaussian input pulse in profile and duration as shown in **Figure 1d**. For comparison, the signal without the control-pulse is also shown, where it temporally broadens to a window of 6 ps and is highly distorted from the original Gaussian profile.

The next signal-pulse example is far from the typical Gaussian shape as shown in **Figure 1e**. However, as in the Gaussian pulse case, the pulse maintained its duration and shape close to

the input profile's parameters. Without the control-pulse the pulse would be highly distorted in shape, stretching out to 5 ps.

We then proceed with the last example which is an asymmetric pulse that is slanted towards positive pulse time, as shown in **Figure 1f**. As with the previous cases, the XPM controlled signal-pulse is close to the input profile at the end of propagation, while the uncontrolled case distorts considerably and stretches to approx. 6 ps.

Interestingly, the effects of the uncontrolled wings of the pulses (see section 1.1 for associated discussion) can be seen as a slightly reduced pulse duration from the input pulse and small amplitude pre/post pulses (below the -4 dB level). This type of error then contributes to primarily to the outcome of pulse compression instead of broadening, desirable for many applications. The dynamics at the temporal edge regions of the control-pulse explains the emergence of these deviations.

The edge locations of the control-pulse are defined when the input signal-pulse goes below an absolute amplitude value of -50 dB. The so-defined decaying edges of the control-pulse introduces a chirp profile that compresses the dispersively chirped temporally broadening wings of the signal-pulse and can even break them into sub-pulses as they interact with it, causing the overall pulse compression.

Also, there is a slight mismatched group-velocity of the signal with control-pulse because of numerical floating-point error. Though small, the mismatch produces XPM induced wavebreaking^[34] that adds small modulations on one side of the pulse profiles. This numerical error also enhances the error from the edge effects.

We provide a video of the second example pulse's propagation across the waveguide in supplementary. The video illustrates the maintained duration and shape of the signal-pulse with control.

Outlook

Other interesting applications emerge if the amplitude of the control-pulse, whose shape is determined by Equation (4) is increased. Instead of just compensating for temporal broadening, the control-pulse acts to nonlinearly compress the signal-pulse, even in dispersive media where temporal self-compression, for example, due to self-phase modulation, is unlikely, i.e., in normal dispersion.

Our calculations indicate that XPM on a signal-pulse can enhance the spectral broadening (e.g., in normal dispersion waveguides) by a factor of $\sqrt{2}$. The temporal compression factor (e.g. in anomalous dispersion waveguides) is also enhanced by the same factor – simply due to this factor of two in the XPM nonlinear coefficient. Thus, using the control-pulse to induce spectral generation through XPM is potentially a highly efficient nonlinear process.

We preliminarily find that simply increasing the amplitude of the found control-pulse from the calculated value given by Equation (4), can induce nonlinear compression of the signal-pulse through the induced additive phase from cross-phase modulation. Thus, the presented method can be used to calculate ideal profiles of control-pulses for XPM on signal-pulses, for the control of such effects as temporal broadening. Also, furthermore, the here presented method could enhance nonlinear bandwidth generation and nonlinear pulse compression in weak amplitude signals.

References

- [1] A. Hasegawa, and F. Tappert, *Appl. Phys. Lett.* **23**, 171–172 (1973).
- [2] D. Grahelj, *Seminar* (2010).
- [3] A. Demircan, S. Amiranashvili, and G. Steinmeyer, *Phys. Rev. Lett.* **106**, 1–4 (2011).
- [4] A. V. Yulin, and D. V. Skryabin, *Phys. Rev. A - At. Mol. Opt. Phys.* **67**, 8 (2003).
- [5] Y. V Kartashov, and V. A. Vysloukh, *Phys. Rev. E* **72**, 26606 (2005).
- [6] K. Luke, Y. Okawachi, M. R. E. Lamont, A. L. Gaeta, and M. Lipson, *Opt. Lett.* **40**, 4823 (2015).
- [7] M. A.G. Porcel, F. Scheppers, J. Epping, T. Hellwig, M. Hoekman, R. G. Heideman, P. J. M. Van der Slot, C. J. Lee, R. Schmidt, R. Bratschitsch, C. Fallnich, K.-J. Boller, *Opt. Express* **25**, (2017).

[8] J. P. Epping, T. Hellwig, M. Hoekman, R. Mateman, A. Leinse, R. G. Heideman, A. van Rees, P. J. M. van der Slot, C. J. Lee, C. Fallnich, and K.-J. Boller, *Opt. Express* **23**, 19596 (2015).

[9] H. Zia, N. M. Lüpken, T. Hellwig, C. Fallnich, and K. J. Boller, *Laser Photonics Rev.* **14**, 1–11 (2020).

[10] J. C. Travers, T. F. Grigorova, C. Brahms, and F. Belli, *Nat. Photonics* **13**, 547–554 (2019).

[11] H. Zia, *Photonics* **8**, 1–18 (2021).

[12] J. W. Choi, B. U. Sohn, G. F. R. Chen, D. K. T. Ng, and D. T. H. Tan, *APL Photonics* **4**, (2019).

[13] H. Chen, Z. Haider, J. Lim, S. Xu, Z. Yang, F. X. Kärtner, and G. Chang, **38**, 4927–4930 (2013).

[14] J. M. Dudley, G. Genty, and S. Coen, *Rev. Mod. Phys.* **78**, 1135–1184 (2006).

[15] A. F. J. Runge, Y. L. Qiang, T. J. Alexander, M. Z. Rafat, D. D. Hudson, A. Blanco-Redondo, and C. M. de Sterke, *Phys. Rev. Res.* **3**, 1–8 (2021).

[16] J. E. Heebner, and R. W. Boyd, *J. Mod. Opt.* **49**, 2629–2636 (2002).

[17] A. M. Steinberg, and R. Y. Chiao, *Phys. Rev. A* **49**, 2071–2075 (1994).

[18] P. Sprangle, J. R. Peñano, and B. Hafizi, *Phys. Rev. E - Stat. Physics, Plasmas, Fluids, Relat. Interdiscip. Top.* **64**, 5 (2001).

[19] J. E. Sharping, Y. Okawachi, and A. L. Gaeta, *Opt. Express* **13**, 6092 (2005).

[20] B. J. Eggleton, C. M. de Sterke, and R. E. Slusher, *J. Opt. Soc. Am. B* **14**, 2980–2993 (1997).

[21] T. B. Pittman, and J. D. Franson, *Phys. Rev. A - At. Mol. Opt. Phys.* **66**, 4 (2002).

[22] P. M. Leung, and T. C. Ralph, *Phys. Rev. A - At. Mol. Opt. Phys.* **74**, 1–6 (2006).

[23] M. N. Islam, G. Sucha, I. Bar-Joseph, M. Wegener, J. P. Gordon, and D. S. Chemla, *J. Opt. Soc. Am. B* **6**, 1149 (2008).

[24] S. Trillo, S. Wabnitz, E. M. Wright, and G. I. Stegeman, *Opt. Lett.* **13**, 871–873 (1988).

[25] N. Nishizawa, and T. Goto, *Opt. Express* **10**, 1151 (2002).

[26] S. F. Wang, A. Mussot, M. Conforti, X. L. Zeng, and A. Kudlinski, *Opt. Lett.* **40**, 3320 (2015).

[27] Z. Deng, J. Liu, X. Huang, C. Zhao, and X. Wang, *Opt. Express* **25**, 28556 (2017).

[28] S. F. Wang, A. Mussot, M. Conforti, A. Bendahmane, X. L. Zeng, and A. Kudlinski, *Phys. Rev. A - At. Mol. Opt. Phys.* **92**, 1–6 (2015).

[29] M. Goutsoulas, V. Paltoglou, and N. K. Efremidis, *J. Opt. (United Kingdom)* **19**, (2017).

[30] G. P. Agrawal, *Applications of Nonlinear Fiber Optics* (2001).

[31] L. B. Michael, M. Ghavami, and R. Kohno, in: *2002 IEEE Conf. Ultra Wideband Syst. Technol. (IEEE Cat. No.02EX580)*: (2002), pp. 47–51.

[32] H. Zia, *Commun. Nonlinear Sci. Numer. Simul.* **54**, (2018).

[33] R. Sollapur, D. Kartashov, M. Zürch, A. Hoffmann, T. Grigorova, G. Sauer, A. Hartung, A. Schwuchow, J. Bierlich, J. Kobelke, M. Chemnitz, M. A. Schmidt, and C. Spielmann, *Light Sci. Appl.* **6**, e17124 (2017).

[34] G. P. Agrawal, P. L. Baldeck, and R. R. Alfano, *Opt. Lett.* **14**, 137–139 (1989).